CLM-P73

United Kingdom Atomic Energy Authority

RESEARCH GROUP

Preprint

DENSITY WAVES IN LOW PRESSURE PLASMA COLUMNS

L. C. WOODS

Culham Laboratory,

Culham, Abingdon, Berkshire

1965

UNCLASSIFIED
(Approved for Publication)

CLM - P 73

DENSITY WAVES IN LOW PRESSURE PLASMA COLUMNS

by

L.C. WOODS*

(To be published in Journal of Fluid Mechanics)

A B S T R A C T

Density waves in low pressure arc discharges have been observed travelling towards the anode with speeds near $(\kappa T_e/M)^{\frac{1}{2}}$. A dispersion relation for these waves is developed, taking into account the boundary effects, namely the continuous loss of ions to the containing walls. This theory is in fair agreement with experiment, except in its prediction of a rather high value for the wave damping. However by allowing for the effect of electrostatic instabilities on anode-approaching waves, due to electron drift, this discrepancy is satisfactorily explained.

* Balliol College, Oxford.

U.K.A.E.A. Research Group,
Culham Laboratory,
Nr. Abingdon,
Berks.

March, 1965 (C/18 ED)

C O N T E N T S

1. INTRODUCTION

Langmuir and Tonks (1929a) were among the first to study the electro-acoustic density waves found in low pressure, mercury arc discharges. They predicted phase velocities close to $(\kappa T_e/M)^{\frac{1}{2}}$, where T_e is the electron temperature and M the ion mass. Since this early work, the problem has been investigated experimentally by several people, including Hatta and Sato (1961), Little (1962), Crawford and Self (1963), and Alexeff and Neidigh (1963); more references are to be found in the recent contribution of Barrett and Little (1965). At low frequencies there are two types of wave in low density plasmas, viz. the 'forward' or electro-acoustic wave with group and phase velocities in the same direction, and the 'backward' or ionization wave with these velocities opposed (Pekárek, 1963). This paper is concerned with the theory of the forward waves, at pressures low enough to make the mean free path for collisions between particles much larger than the discharge radius.

The experiments on forward waves (Barrett and Little, 1965) reveal two interesting points, viz. (i) that the waves appear to have a cut-off frequency below which they are evanescent, and (ii) that only anode-approaching waves are readily observed. The waves are damped by ion collisions with the walls containing the discharge, and as damping is known in other wave propagation problems to eliminate a sharp cut-off (e.g. see Woods, 1962, Jephcott and Malein, 1964), it seems likely that waves exist at all frequencies, but that those in the experimentally found cut-off range are too heavily damped to be observable. In fact a rough estimate of the damping by wall collisions gives such a high value that it is surprising that any waves are observed at all. Bickerton (unpublished) and Little (1962) have provided a qualitative explanation of this point and also of (ii) above, by pointing out that the electron drift speeds towards the anode are high enough to excite electrostatic instabilities (Stringer, 1964). This effect reduces, and may even eliminate, the damping for anode-approaching waves, but augments the damping of cathode directed waves.

We shall deal with a cylindrical discharge having constant steady-state properties along its length, say the Oz-direction. Of course the steady state solution needs to be known before the theory of small, wave-like perturbation can be developed. Let n_{es}, n_{is} denote the steady-state electron and ion densities, and let φ_s be the corresponding electrostatic potential, then the Tonks-Langmuir theory (1929b) gives these numbers as functions of the radius r from the discharge axis. In this theory the whole radial interval $(0,r_o)$ is divided into an inner region in which $n_{es} = n_{is}$ and a thin sheath near the wall in which the charge density is not zero. In most experiments this sheath is thin enough to be neglected; we shall do this and set $n_e = n_i = n$, say, for both steady and unsteady motions. Then on assuming an isothermal discharge, we can integrate Ohm's law to find that

$$n = n_a n^{-\eta}, \qquad \eta \equiv -e\varphi/\kappa T_e \qquad \ldots(1)$$

for steady and unsteady arcs. The rate at which ions are generated per unit volume will be put equal to azn, where z is a constant and $a \equiv (\kappa T_e/M)^{\frac{1}{2}}$, then for this case Tonks and Langmuir find the integral equation

$$\sqrt{2}\,\exp(-\eta_s) = \frac{z}{r}\int_o^r r'\left\{\eta_s(r) - \eta_s(r')\right\}^{-\frac{1}{2}} \exp\left\{-\eta_s(r')\right\} dr',$$

for the steady state. This is solved numerically, and then the boundary condition $d\eta_s/dr = \infty$ at $r = r_o$ gives the eigenvalue

$$zr_o \approx 1.092 \qquad \ldots(2)$$

This exact integral-equation treatment of the steady state is not at all easy to extend to the unsteady case, and so in the next section we give an approximate differential-equation formulation of the problem not having this disadvantage. The somewhat involved second-order differential equation for the perturbation ion velocities that follows, is solved numerically to give the dispersion relation $F(\omega,k) = 0$, where ω is a real frequency and k a complex wave number, $k = k_R + ik_I$.

Finally Stringer's (1964) theory of electrostatic instabilities is used to modify the damping length k_I^{-1}, and so predict the conditions under which growing waves can be expected.

2. APPROXIMATE THEORY

Let f_j ions have the velocity $\underset{\sim}{u}_j$, and write

$$\underset{\sim}{v} \equiv \sum_j f_j \underset{\sim}{u}_j/n, \qquad n \equiv \sum_j f_j, \qquad \ldots (3)$$

then conservation of mass and momentum of the ions gives

$$\frac{\partial n}{\partial t} + \nabla \cdot (n\underset{\sim}{v}) = azn \qquad \ldots (4)$$

and

$$\frac{\partial}{\partial t}(n\underset{\sim}{v}) + \nabla \cdot (n\underset{\sim}{\underset{\sim}{v}}) = -\frac{1}{M}(\nabla . \underset{\approx}{p}_i + e\nabla\varphi), \qquad \ldots (5)$$

where

$$\underset{\approx}{p}_i \equiv \sum_j f_j (\underset{\sim}{u}_j - \underset{\sim}{v})(\underset{\sim}{u}_j - \underset{\sim}{v}),$$

is the ion pressure tensor relative to the drift velocity $\underset{\sim}{v}$. The approximation we shall use is simply

$$\underset{\approx}{p}_i = 0, \qquad \ldots (6)$$

which will be justified later for the steady arc discharge. Then by (1), (4) and (6), (5) can be written

$$(\frac{\partial}{\partial t} + \underset{\sim}{v}.\nabla)\,\underset{\sim}{v} + azn = a^2\,\nabla\eta. \qquad \ldots (7)$$

Let $\underset{\approx}{\zeta} \equiv \nabla\times\underset{\sim}{v}$ be the vorticity, and $\frac{d}{dt} \equiv \frac{\partial}{\partial t} + \underset{\sim}{v}.\nabla$ be the rate of change following the motion, then the curl of (7), viz.

$$\frac{\partial \underset{\approx}{\zeta}}{\partial t} - \nabla \wedge (\underset{\sim}{v} \wedge \underset{\approx}{\zeta}) + az\underset{\approx}{\zeta} = 0,$$

can, with the aid of (4), be arranged in the form

$$\frac{d}{dt}\left(\frac{\underset{\approx}{\zeta}}{n}\right) = \left(\frac{\underset{\approx}{\zeta}}{n}\right) \cdot \nabla \underset{\sim}{v} \qquad \ldots (8)$$

From this result we draw the conclusion, familiar in classical fluid mechanics, that a fluid element initially without vorticity never acquires any (Stokes' theorem). In the steady state $\underset{\sim}{v}$ is entirely radial, so $\underset{\approx}{\zeta}_s = 0$. And if we now assume that the unsteady motions are generated smoothly from this steady state, it follows that

$$\nabla \wedge \underset{\sim}{v} = 0. \qquad \ldots (9)$$

Turning now to the steady state, so that we may have a comparison with the exact Tonks-Langmuir theory, we find from (1), (4) and (7) that

$$\begin{aligned} (rn_s u)'/r &= zn_s, \\ zu + uu' &= \eta_s' = -n_s'/n_s, \end{aligned} \qquad \ldots (10)$$

where $u \equiv v_s/a$ and the dashes denote radial derivatives. Let $x \equiv r/r_o$, then from (10) we find the non-linear equation

$$\frac{du}{dx} = \frac{zr_o(1+u^2) - u/x}{1 - u^2}, \qquad \ldots (11)$$

which has been solved numerically, see Table 1. It is found that at $u = 1$, where du/dx and η_s' are infinite, $zr_o x \approx 1.109$, and so following Tonks and Langmuir, we can put the wall at $x = 1$ provided z satisfies

$$\alpha \equiv zr_o \approx 1.109, \qquad \ldots (12)$$

which is remarkably close to the exact value given in (2). A very close fit to the numerical solution given in the Table is

$$u = 1 - \sqrt{(1 - x)}. \qquad \ldots (13)$$

which gives $n_s(r)$ differing by only a few per cent from the T-L theory.

As a further check on the approximation $\underset{\approx}{p}_i = 0$, the author has considered ions created throughout the volume and falling radially through a parabolic

potential distribution. In this case

$$\sum_j (f_j u_j)^2 \approx \frac{8}{9} n \sum_j f_j u_j^2 ;$$

our approximation replaces 8/9 by unity, so we might expect a 10% error to be introduced at this point.

3. PERTURBATION THEORY

Let $n(\underset{\sim}{r},t) = n_s(\underset{\sim}{r}) + n_1(\underset{\sim}{r}) \exp\{i(kz + m\theta - \omega t)\}$, with similar forms for $\underset{\sim}{v}$ and η, then from (1) and (4)

$$n_1 = - n_s \eta_1, \qquad \ldots (13)$$

$$- i\omega n_1 + \nabla . (n_1 v_s \underset{\sim}{\hat{r}} + n_s \underset{\sim}{v}_1) = azn_1, \qquad \ldots (14)$$

where $\underset{\sim}{\hat{r}}$ is unit vector in the radial direction. Let

$$\mathcal{L} \equiv -i \frac{\omega}{a} + u \frac{\partial}{\partial r} , \qquad \ldots (15)$$

then on using (10) to eliminate some terms, we can write (14) in the form

$$\mathcal{L} \left(\frac{n_1}{n_s} \right) + \left(\frac{n_s'}{n_s} + \frac{1}{r} \frac{d}{dr} r \right) \frac{v_{1r}}{a} + ik \frac{v_{1z}}{a} + \frac{im}{r} \frac{v_{1\theta}}{a} = 0. \qquad \ldots (16)$$

The linear perturbation form of (7), plus (13), give

$$\begin{aligned} (u' + z + \mathcal{L}) \frac{v_{1r}}{a} + \left(\frac{n_1}{n_s} \right)' &= 0, \\ (z + \mathcal{L}) \frac{v_{1z}}{a} + ik \frac{n_1}{n_s} &= 0, \end{aligned} \qquad \ldots (17)$$

and

$$\left(\frac{u}{r} + z + \mathcal{L}\right) \frac{v_{1\theta}}{a} + \frac{im}{r} \frac{n_1}{n_s} = 0.$$

It is easily verified that these equations are satisfied by

$$v_{1z}' = ik\, v_{1r}, \qquad m\, v_{1z} = kr\, v_{1\theta} , \qquad \ldots (18)$$

which are two of the components of the perturbation form of (9). (The third component is an identity.) Then using (17) and (18) to eliminate n_1, v_{1r} and $v_{1\theta}$ from (16), we arrive at

$$(1-u^2)\frac{d^2w}{dx^2} + \frac{1}{x}\left\{1 - 2xu\left(\frac{du}{dx} + \alpha - i\sigma\right)\right\}\frac{dw}{dx} - \left(h^2 + \frac{m^2}{x^2} - \sigma^2 - i\sigma\alpha\right)w = 0, \quad \ldots (19)$$

where α is defined in (12) and

$$w \equiv v_{1z}/a, \qquad h \equiv r_o k = h_R + ih_I, \qquad \sigma \equiv \omega r_o/a. \qquad \ldots (20)$$

At $r = r_o$ Maxwell's slip-type boundary condition reduces to $dw/dx = 0$, a result that is not affected by the fact that the particles are charged in our application (Luzzi and Gross 1964). This condition also follows directly from (19), because at $r = r_o$ du/dx is infinite so that $(dw/dx)_{ro}$ must vanish for w to remain finite at the boundary. At the axis the solution must be finite and continuous; in this neighbourhood $u = 0$ and (19) reduces to Bessel's equation for which the appropriate axial boundary conditions are $m \neq 0$, $w = 0$, and $m = 0$, $dw/dx = 0$ (cf. the singularities in the last two terms of (19)). Summarizing, we have

$$\begin{matrix} & w = 0 & \text{if} & m \neq 0 & & & \\ r = 0; & & & & : & r = r_o; & \dfrac{dw}{dx} = 0. \\ & \dfrac{dw}{dx} = 0 & \text{if} & m = 0 & & & \end{matrix} \qquad \ldots (21)$$

The solution of (19) for given σ, subject to (21) is possible only for a particular value of h, and the relation between h and σ so determined is the required dispersion relation. When w has been found, the number density follows from (17), which can be written

$$\frac{n_1}{n_s} = \frac{1}{h}\left(\sigma + i\alpha + iu\frac{d}{dx}\right) w. \qquad \ldots (22)$$

4. THE SOLUTION

The problem defined by (19) and (21) has been solved numerically for the cases $m = 0$ and $m = 1$, and for several radial modes in each case. As the

higher radial modes are strongly damped, this calculation need not be extended beyond the second radial mode.

Notice that if m is zero, w = constant satisfies (19) and (21) provided $h^2 = \sigma^2 + i\sigma\alpha$, i.e.

$$h_R = \sigma \left\{ \tfrac{1}{2} + \tfrac{1}{2} \left[1 + \left(\frac{\alpha}{\sigma} \right)^2 \right]^{\frac{1}{2}} \right\}^{\frac{1}{2}}, \quad h_I = \frac{\alpha\sigma}{2 h_R}. \qquad \ldots (23)$$

When $\sigma \gg \alpha$, $h_R \approx \sigma$, $h_I \approx 0.55$. We shall label this case the zeroth radial mode of $m = 0$. The values of h_R, h_I for the first mode - the $(0,1)$ mode, say - are set out in Table 2, which also includes the $(1,1)$ and $(1,2)$ modes.

Fig.1 shows the (σ, h_R) relation for the first two radial modes with $m = 0$, while Fig.2 contains the (h_I, σ) curves for $m = 0$ and 1, and shows the severity of damping. For example, in a 5 cm diameter tube the damping length for the $(0,1)$ mode at $\sigma = 6$ is $2.5/1.6 \approx 1.7$ cms. Figs.3a and 3b show the radial distributions for the perturbation amplitude, and for the phase angle relative to the axial disturbance, both for the $(0,1)$ mode. There is no particular relation between the relative amplitudes in Fig.3a for differing values of σ.

The experimental points shown in Fig.1 are taken from Barrett and Little (1965), the notation used for the points being the one adopted by them. The method of exciting the waves produces a $m = 0$ mode, and this is confirmed by measurements of $|n_1|$ as a function of radius. These latter measurements show sufficient radial variation to enable us to rule out the simple $(0,0)$ mode in which $|n_1| \propto n_s$ (cf. equation (22)). And taking Fig.1 into account it is a reasonable conclusion that the waves belong to the $(0,1)$ mode, and that the theory predicts the phase velocity, ω/h_R, fairly accurately. However the damping is another matter, a problem we shall return to in Section 5.

Very few measurements of radial variation of $|n_1|$ have been made; they are difficult to make, and perhaps at this stage not too much should be made of the disagreement between the experimental points shown in Fig.3a for $\sigma = 3.65$ and the trend of the $\sigma = 4$ curve. The experimental points shown are actually average

TABLE 1

STEADY STATE SOLUTION

$zr_o x$	0.1	0.2	0.3	0.4	0.5	0.6
u	0.0501	0.1008	0.1526	0.2064	0.2630	0.3236
$zr_o x$	0.7	0.8	0.9	1.0	1.0321	1.0583
u	0.3900	0.4652	0.5546	0.6722	0.7222	0.7722
$zr_o x$	1.0788	1.0938	1.1037	1.1087	1.1088	1.1089
u	0.8222	0.8722	0.9222	0.9722	1.0000	1.0222

TABLE 2

DISPERSION RELATION

Mode	(0,1)		(1,1)		(1,2)	
σ	h_R	h_I	h_R	h_I	h_R	h_I
0	0.000	3.633	0.000	1.976	0.000	4.984
0.5	0.147	3.595	0.247	1.924	0.123	4.955
1.0	0.305	3.481	0.537	1.773	0.251	4.866
1.5	0.488	3.286	0.925	1.548	0.390	4.716
2.0	0.719	3.003	1.439	1.332	0.549	4.500
2.5	1.037	2.633	2.021	1.192	0.739	4.211
3.0	1.504	2.209	2.608	1.116	0.981	3.843
3.5	2.144	1.840	3.184	1.076	1.310	3.394
4.0	2.868	1.605	3.747	1.056	1.781	2.888
4.5	3.588	1.479	4.302	1.050	2.433	2.411
5.0	4.283	1.417	4.849	1.053	3.207	2.062
5.5	4.954	1.393	5.390	1.065	4.004	1.844
6.0	5.607	1.394	5.925	1.087	4.781	1.708
6.5	6.248	1.415	6.453	1.121	5.535	1.617
7.0	6.882	1.452	6.971	1.173	6.276	1.544
7.5	7.514	1.504	7.465	1.261	7.021	1.461
8.0	8.149	1.570	8.003	1.495	7.711	1.249

values at opposite points of a diameter, and discrepencies of up to 50% in these two values can occur. Experimental values of $\arg(n_1)$ as a function of radius are also somewhat variable. They reveal an average lag of about 120^o between the axis and the wall at $\sigma \approx 4$, which is in agreement with the theoretical value shown in Fig.3b.

5. THE WAVE DAMPING

Few measurements of wave damping are available. Little (unpublished) has found values of h_I of about 0.25 for $3 < \sigma < 5$, while Barrett and Little found that for $\sigma \geqslant 5$ the waves were virtually undamped, and sometimes even growing. These remarks apply only to anode-approaching waves. Now even the (0,0) mode has twice the damping found by Little, and so we are forced to invoke the electrostatic instabilities, as described in the Introduction, to explain this discrepancy. The result we require is contained in Stringer's (1964) paper on this subject. For small T_i/T_e and small kV_e/Ω_e, where V_e is the electron drift speed and Ω_e the Langmuir frequency, Fig.1b of the paper provides the growth rate $\gamma \approx 0.62\, k_R V_e (m_e/m_i)^{\frac{1}{2}}$, a value that Dr Stringer has kindly confirmed. This is the case encountered in the experiments. Combining this with the theory given above, we find the net damping coefficient, say k_I^*, to be $k_I \pm \gamma k_R/\omega$, the positive (negative) sign for cathode-approaching (anode-approaching) waves. This result can be expressed in the form

$$h_I^* = h_I\,(1 \pm g), \qquad g \equiv 0.62 \left(\frac{v_e}{c_e}\right) \frac{h_R^2}{\sigma h_I}, \qquad \ldots (24)$$

where $c_e \equiv (xT_e/m_e)^{\frac{1}{2}}$.

In Fig.4 we have plotted that part of g given by the theory of this paper. For a typical experiment reported by Barrett and Little, $V_e \approx j/en = 2.8 \times 10^7$cms/sec, and $c_e \approx 8 \times 10^7$cms/sec, whence $g = 0.22\,(h_R^2/\sigma h_I)$. From Fig.4 we find that $h_I = 0.25$ at $\sigma = 6$, and instability ($g > 1$) occurs for $\sigma \geqslant 7$. This theory is, of course, no more than semi-empirical, for Stringer's work strictly applies only to a uniform, unbounded plasma, and also the theory given in Sections 2-4 neglects

drift velocities and currents. However our superposition of the two theories does provide at least a qualitative explanation of the observations.

6. ACKNOWLEDGEMENTS

Drs P.F. Little and R.J. Bickerton of Culham Laboratory, Berkshire have helped me in many discussions of the problem studied in this paper. I am also indebted to Dr C. Phellps of the Oxford University Computing Laboratory for the computer calculations on which the results of Section 4 depend.

7. REFERENCES

ALEXEFF, J. and NEIDIGH, R.V. Phys. Rev., vol.129, no.516 (1963).

BARRETT, P.J. and LITTLE, P.F. Phys. Rev. Lett. (1965).

CRAWFORD, F.W. and SELF, S.A. Proc. Sixth Int. Conf. Ionization Phenomena (Paris) vol.3, no.129 (1963).

HATTA, Y. and SATO, N. Proc. Fifth Int. Conf. Ionization Phenomena (Munich), vol.1, no.478 (1961).

JEPHCOTT, D.F. and MALEIN, A. Proc. Roy. Soc. A, vol.278, no.243 (1964).

LITTLE, P.F. Nature, vol.194, no.1137 (1962).

LUZZI, T.E. and GROSS, R.A. Physics of Fluids, vol.7 (8), no.1329 (1964).

PEKAREK, L. Proc. Sixth Int. Conf. Ionization Phenomena (Paris), vol.3, no.367, (1963).

STRINGER, T.E. Plasma Phys.(J. Nucl. Energy, Pt. C), vol.6, no.267 (1964).

TONKS, L. and LANGMUIR, I. Phys. Rev. vol.33, no.195 (1929a).

TONKS, L. and LANGMUIR, I. Phys. Rev. vol.34, no.876 (1929b).

WOODS, L.C. J. Fluid Mech. vol.13 (4), no.570 (1962).

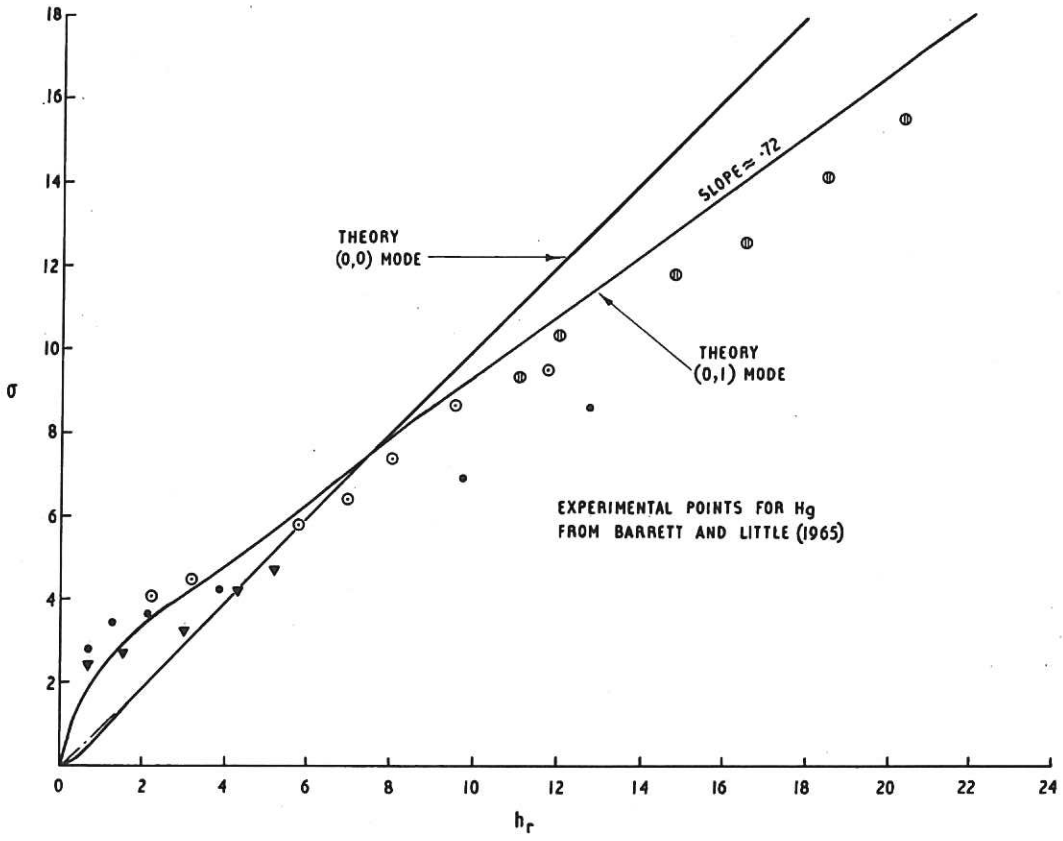

Fig. 1 The dispersion curve (CLM-P73)

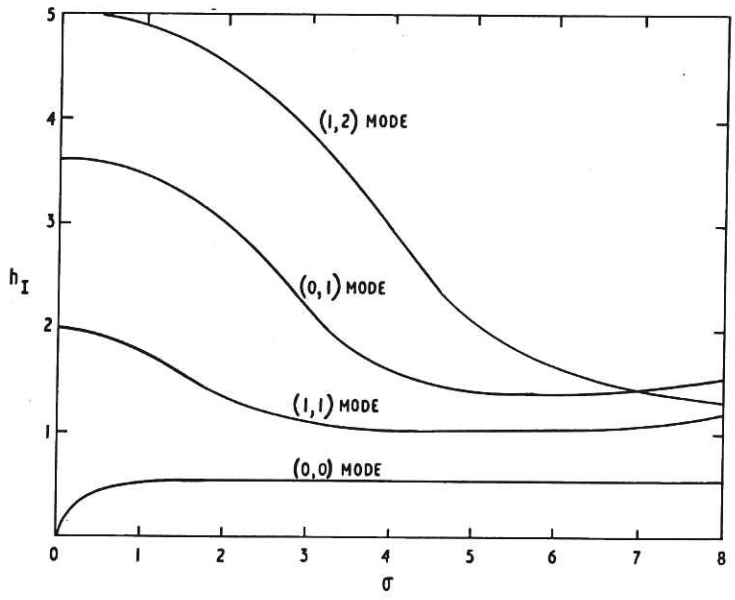

Fig. 2 Damping due to wall losses (CLM-P73)

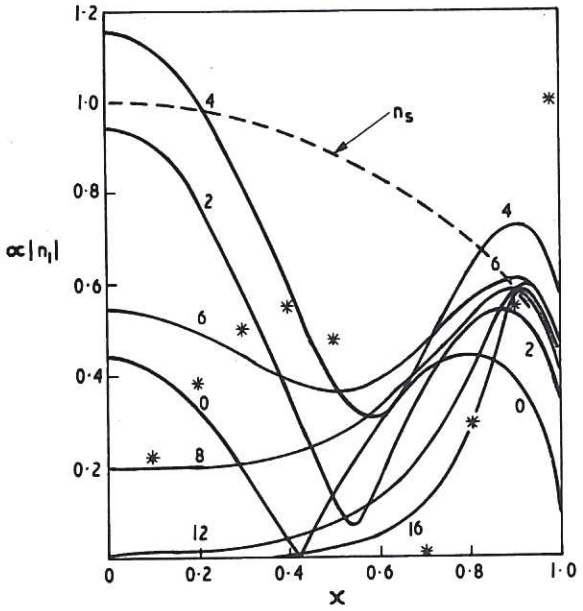

Fig. 3a (CLM-P73)
Radial distribution of perturbation amplitude for various values of σ

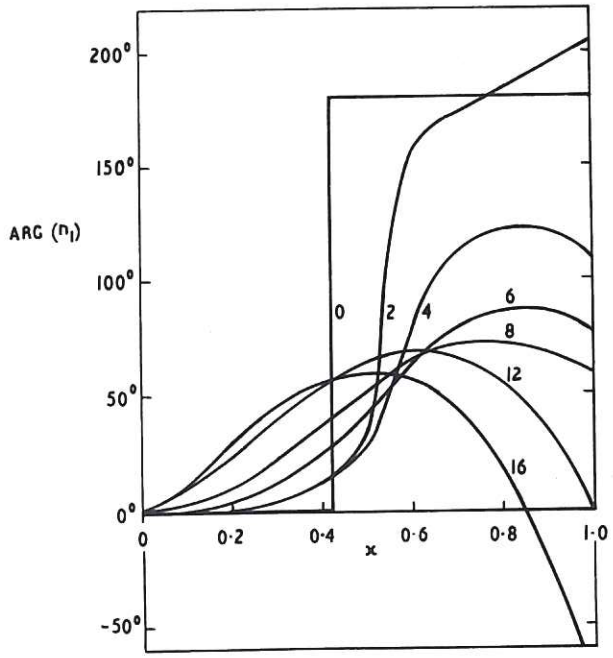

Fig. 3b Phase lag in wave (CLM-P73)

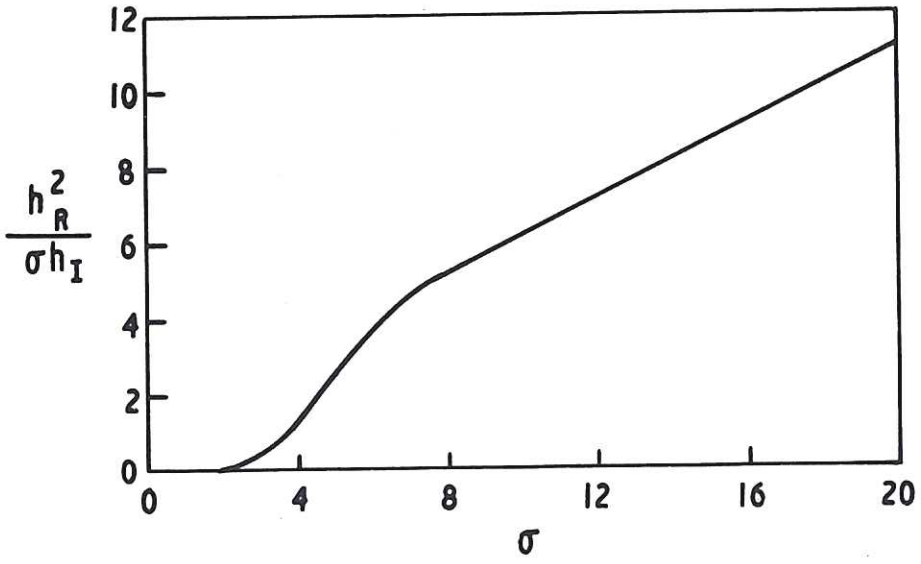

Fig. 4 Damping parameter (CLM-P73)